(International Print/Online Journal)

SJIF IMPACT FACTOR: 6.829
PUBMED-National Library of Medicine ID-101739732

ISSN (Print): 2209-2870
ISSN (Online): 2209-2862

International Journal of Medical Science and Current Research (IJMSCR)
Available online at: www.ijmscr.com
Volume 9, Issue 2 , Page No: 419-427
March-April 2026

IJMSCR

In Silico Modelling and Validation of Rabphilin-3A-Like Isoform CRA_b (EAW90671) Implicated in Alzheimer's and Huntington's

Rajneesh Prajapat [1], Ashwini Praveen Khairkar [2], Praveen Khairkar [3]
[1,2]Department of Biochemistry, [3]Department of Psychiatry & Clinical Neuroscience,
Pacific Institute of Medical Sciences, Sai Tirupati University, Udaipur, Rajasthan, India

***Corresponding Author:**
Rajneesh Prajapat
Department of Biochemistry, Pacific Institute of Medical Sciences,
Sai Tirupati University, Udaipur, Rajasthan, India

Type of Publication: Original Research Paper
Conflicts of Interest: Nil

Abstract

Background: Rabphilin-3A-like (RPH3AL), a member of the Rab effector protein family, plays a critical role in regulated membrane trafficking and synaptic vesicle exocytosis in neurons and neuroendocrine cells. Loss or dysfunction of Rabphilin-3A–associated proteins has been implicated in synaptic failure, a key pathological feature of Alzheimer's disease and Huntington's disease. Structural characterization of RPH3AL isoforms is therefore essential for understanding disease mechanisms and enabling structure-based drug discovery. *Aim:* This study aimed to perform *in silico* structural characterization of Rabphilin-3A-like isoform CRA_b (EAW90671) and RPH3AL (AIC55601) using homology modelling and comprehensive structural validation. *Materials and Methods:* Protein sequences of Rabphilin-3A-like isoform CRA_b (EAW90671) and RPH3AL (AIC55601) were retrieved from the NCBI database. Homology models were generated using the SWISS-MODEL server based on suitable templates from the Protein Data Bank. Structural validation and quality assessment were performed using PROCHECK, ProSA, and QMEAN scoring functions. *Results:* The generated models demonstrated high stereochemical quality, with 94.23% and 93.48% of residues of EAW90671 and AIC55601, respectively, located in the most favoured regions of the φ-ψ (Ramachandran) plot. ProSA Z-scores (−3.89 for EAW90671 and −1.89 for AIC55601) and QMEAN Z-scores (−2.57 and −1.43, respectively) indicated acceptable overall model quality and structural reliability. Comparative analysis showed significant structural similarity with the experimentally determined Rabphilin-3A structure from *Rattus norvegicus* (PDB ID: 1ZBD_B). *Conclusion:* The *in silico* modelling and validation results indicate that the predicted 3D structures of Rabphilin-3A-like isoform CRA_b and RPH3AL are reliable and biologically plausible. These structural models provide a valuable framework for future structure-based drug design and therapeutic exploration targeting synaptic dysfunction in Alzheimer's and Huntington's diseases.

Keywords: RPH3AL, Alzheimer's disease; Huntington's disease, φ-ψ plot, ProSA

Introduction

Rabphilin-3A-like (RPH3AL), encoded by the *Rabphilin-3A-like* (*RF3* or *RPH3A*) gene, is a member of the Rab effector protein family that plays a pivotal role in regulated membrane trafficking and vesicle fusion events. Proteins of this family interact with Rab GTPases and are essential for synaptic vesicle docking, priming, and calcium-dependent exocytosis, particularly in neurons and neuroendocrine cells [1,2]. Rabphilin-3A-related proteins are also implicated in maintaining postsynaptic receptor stability, thereby contributing to synaptic plasticity and efficient neurotransmission.

Rabphilin-3A and its related isoforms are characterized by conserved C2 domains that mediate calcium- and phospholipid-dependent interactions with synaptic membranes. Through these structural motifs, RPH3AL participates in fine-tuning neurotransmitter release and synaptic vesicle recycling [3,4]. Disruption of these processes is known to impair synaptic homeostasis, a hallmark of several neurodegenerative disorders.

Growing evidence links altered expression or loss of Rabphilin-3A-associated proteins with neurodegenerative diseases, notably Alzheimer's disease and Huntington's disease. Synaptic dysfunction precedes overt neuronal loss in both conditions, and defects in vesicle trafficking and exocytosis are increasingly recognized as early pathogenic events [5,6]. The association of RPH3A loss with these disorders underscores the importance of detailed structural and functional characterization of its isoforms to better understand disease mechanisms and to identify potential therapeutic targets.

Among the known isoforms, Rabphilin-3A isoform CRA_b (EAW90671) remains poorly characterized at the structural level. Experimental determination of protein structure is often time-consuming and costly, making computational approaches such as homology modelling and *in silico* analyses valuable alternatives. Structure-based *in silico* drug design enables the identification of functional domains, binding pockets, and potential ligand interactions, thereby accelerating early-stage therapeutic discovery [7,8].

Aim and Objectives

The present study aim to characterize the Rabphilin-3A-like (RF3 or RPH3A) encoded protein RPH3AL (AIC55601), with specific emphasis on isoform CRA_b (EAW90671), using homology modelling, structural validation, and *in silico* drug designing approaches. This work seeks to provide a computational framework for understanding the structural features of RPH3AL relevant to synaptic function and its potential involvement in Alzheimer's and Huntington's diseases, thereby supporting future structure-based therapeutic strategies.

Materials and Methods

Retrieval of Genome Sequence: The sequence of *Rabphilin-3A-like* (*RF3* or *RPH3A*) retrieved from NCBI database. The CDS protein sequences of RPH3AL (KJ898037) were selected for homology modeling based structural analysis and validation e.g., rabphilin 3A-like (without C2 domains), isoform CRA_b [*Homo sapiens*]: EAW90671.

Homology Modeling: FASTA sequence of Rabphilin 3A-like (without C2 domains) [EAW90671] and RPH3AL (AIC55601) was align separately with PDB database using NCBI-BLASTp. The significant alignments with maximum identity selected for homology modelling. All the homologous protein structures were downloaded from Protein Data Bank (PDB). The SWISS-MODEL server was used for homology-modelling. The pdb files of CDS were retrieved from SWISS-MODEL server and homologous from PDB, were used for 3D structure designing, modeling and validation.

Model Reputation: The UCLA-DOE server used for the quality analysis of protein crystal structure [9] and PROCHECK server used for validation of structure model [10]. The results of analysis suggesting reliability of model [11]. The overall G-factor, residue positions in φ-ψ plot regions analysis was used for the selection of suitable model [12,13]. The protein stability was analyzed by using QMEAN (version 3.1.0) [14, 15] and ProSA Z-score [16, 17, 18, 20, 21].

The research project was approved by the Ethics Committee (Registration no. STU/IEC/2026/005) of Pacific Institute of Medical Sciences, Sai Tirupati University, Udaipur, Rajasthan, India.

Results

Protein Model Building: The alignment between target and template was performed by using homology modeling [22]. The 3D ribbon model Rabphilin 3A-like (without C2 domains) [EAW90671], and RPH3AL (AIC55601) was generated using 3D structure server (https://swissmodel.expasy.org/assess) (Fig. 1a,b).

Volume 9, Issue 2; March-April 2026; Page No 419-427

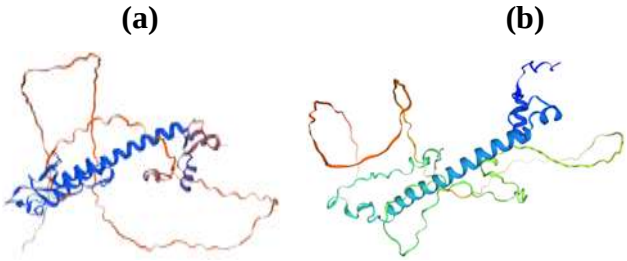

Figure 1: 3D ribbon structure model of Rabphilin-3A-like (RF3 or RPH3A) proteins: [a] Rabphilin 3A-like (without C2 domains) [EAW90671], [b] RPH3AL (AIC55601) generated using 3D assessment server.

Model Reputation: Rabphilin 3A-like (without C2 domains) [EAW90671] model corresponding to probability conformation with 94.23%% residues of favoured section, outliers (2.13%), in generously allowed regions of φ-ψ plot. The RPH3AL (AIC55601) model corresponding to probability conformation with 76.41% residues of favoured section, outliers (9.86%), Clash Score 0.69, and MolProbity Score 1.98 residue of outer section in φ-ψ plot [23] (Fig. 2a,b; Table 1). The above results indicate the reliability of protein models [24, 25].

The φ-ψ plot statistics of Rabphilin 3A-like (without C2 domains) [EAW90671] and The RPH3AL (AIC55601) explained in table 1.

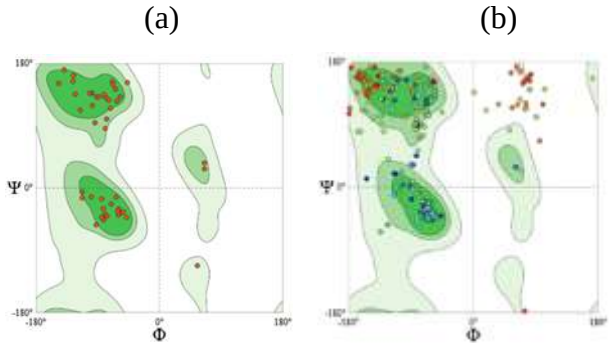

Figure 2: (a) φ-ψ plot of [a] Rabphilin 3A-like (without C2 domains) [EAW90671]: Total number of residues were (94.23%) in favoured [A, B, L], (5.77%) in allowed [a,b,l,p] and, (2.13%) in generously allowed regions. (b) φ-ψ plot of [b] RPH3AL (AIC55601): Total number of residues were (93.48%) in favoured [A, B, L], 6.52 in allowed [a,b,l,p] and, 0 (0.0%) in disallowed regions.

Significant alignments using p-BLAST of surface Rabphilin 3A-like (without C2 domains) [EAW90671] displays maximum similarity with Chain B (RABPHILIN-3A) [Rattus norvegicus]1ZBD_B (60.94% identity) and RPH3AL (AIC55601) also show significant alignment with Chain B, RABPHILIN-3A [Rattus norvegicus] (1ZBD_B) (46.09% identity). The 3D structure (Fig and pdb file of 1ZBD_B was retrieved from PDB for homology modeling-based structure analysis and validation (Fig 3a).

Figure 3: 3D ribbon structure model of Chain B, RABPHILIN-3A [Rattus norvegicus] (1ZBD_B)

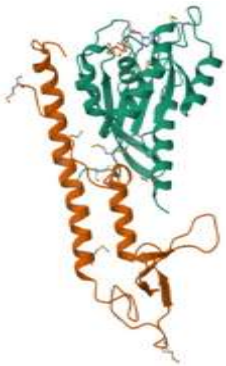

Volume 9, Issue 2; March-April 2026; Page No 419-427

Figure 4: 2D [a] and 3D [b] φ-ψ / Ramachandran plot of Chain B, RABPHILIN-3A [Rattus norvegicus] (1ZBD_B): Total number of residues were 248 (93.23%) in favoured [A, B, L], 14 (5.26%) in allowed [a,b,l,p] and, 4 residues in disallowed (1.50%) region.

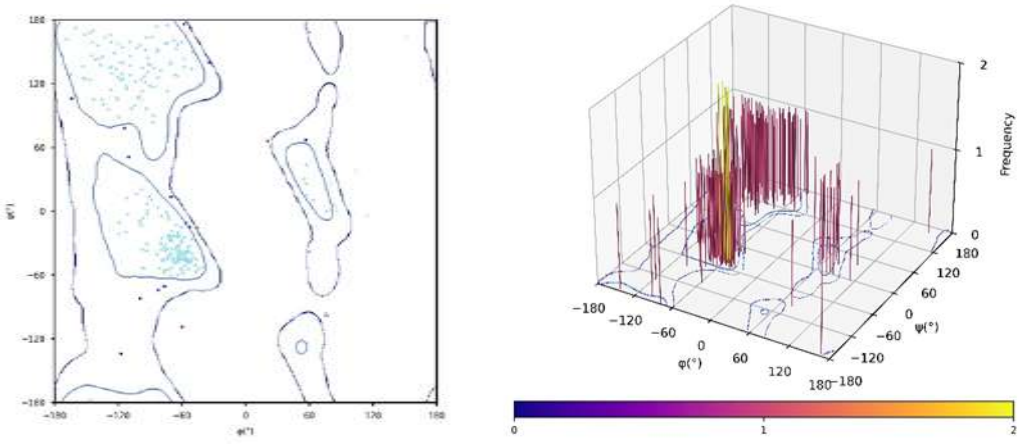

The Rabphilin 3A-like (without C2 domains) [EAW90671] model corresponding to probability conformation with 94.23 % in favoured, 5.77 % in allowed and, 0.00 %) in disallowed regions of φ-ψ plot. The RPH3AL (AIC55601) model corresponding to probability conformation with 93.48% residue of core section, 6.52% of allowed section and 0.0 % residue of outer section in φ-ψ plot [23] (Fig. 2a,b; Table 1). The above results indicate the reliability of protein models [24]. Significant alignments using p-BLAST of Rabphilin 3A-like (without C2 domains) [EAW90671] displays maximum similarity with Chain B (RABPHILIN-3A) [Rattus norvegicus]1ZBD_B (60.94% identity) and RPH3AL (AIC55601) show significant alignment with similar Chain B, RABPHILIN-3A [Rattus norvegicus] (1ZBD_B) (46.09% identity) were retrieved from PDB for homology modeling-based structure analysis and validation.

Based on the analysis of 118 structures of resolution of at least 2.0 Å and R-factor no greater than 20%, a good quality model would be expected to have over 90% in the most favoured regions. All selected sequences have more than 90% residues in Favoured regions [A, B, L] of φ-ψ plot, that indicates good quality of models (Table 1).

Table 1: The φ-ψ plot regions of Rabphilin 3A-like (without C2 domains) [EAW90671], RPH3AL (AIC55601), and Chain B (RABPHILIN-3A) [Rattus norvegicus]1ZBD_B.

φ-ψ Plot regions	EAW90671	AIC55601	1ZBD_B
	%	%	%
Favoured regions [A, B, L]	94.23	93.48	93.21
Allowed regions [a, b, l, p]	5.77	6.52	5.26
Disallowed regions	0.00	0.0	1.50
C-Beta Deviations	2	2	2
Bad Bonds	1 / 407	0 / 371	1/266
Bad Angles	4 / 543 (A133 ARG-A134 PRO), (A128 SER-A129 PRO),	2 / 492 (Y107 SER-Y108 SER)	-

Volume 9, Issue 2; March-April 2026; Page No 419-427

	(A124 GLY-A125 ILE), (A108 SER-A109 SER)		

Validation of Model: ProSA was used to figure out potential errors in 3D model of Rabphilin 3A-like (without C2 domains) [EAW90671], RPH3AL (AIC55601) and RABPHILIN-3A [Rattus norvegicus] (1ZBD_B) CDS. The archived ProSA Z-score score -3.89, -1.89, and -6.15 for Rabphilin 3A-like (without C2 domains) [EAW90671], RPH3AL (AIC55601) and RABPHILIN-3A [Rattus norvegicus] (1ZBD_B) respectively indicates two aspects, overall model quality and energy deviation (Fig. 5-7).

The predicted values of Z-score indicate less erroneous structures [20, 25]. Reliability of projected model based on scoring function of QMEAN that stated as 'Z-score' (Fig. 6-9) [10, 26].

Figure 5: ProSA service examination of Rabphilin 3A-like (without C2 domains) [EAW90671] overall model quality (a) and local model quality (b) Z-Score -3.89.

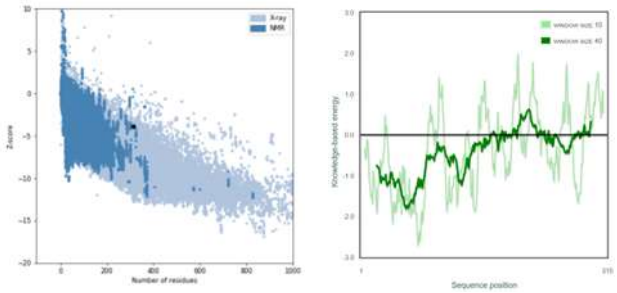

Figure 6: ProSA service examination of RPH3AL (AIC55601) overall model quality (a) and local model quality (b) Z-Score -1.89.

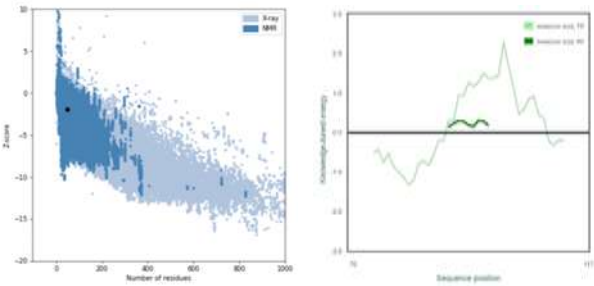

Figure 7: ProSA service examination of pdb homologous Chain B, RABPHILIN-3A [Rattus norvegicus] (1ZBD_B) overall model quality (a) and local model quality (b) Z-Score -6.15.

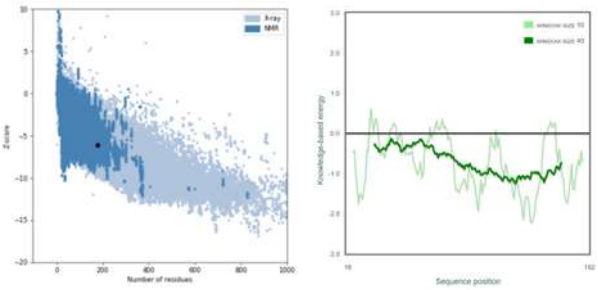

Volume 9, Issue 2; March-April 2026; Page No 419-427

The QMEAN scores -2.57, -1.43, 0.06 and -2.84 for biological unit reference set of Rabphilin 3A-like (without C2 domains) [EAW90671], RPH3AL (AIC55601) and RABPHILIN-3A [Rattus norvegicus] (1ZBD_B) respectively, that is very close to 0 and its illustrations acceptable values [28]. Assessed validity of model predictable among 0 and 1, that could be concluded from the density plot locus set for QMEAN score (Fig. 8-10). Figure 8 to 10, illustrations QMEAN scores for biological unit reference set that used as a tool for oligomeric protein assessment.

We have applied QMEAN Z-scores to experimental structures from the PDB database [27]. Table 2 show the Z-scores analysis of two experimental structures solved by X-ray diffraction of Rabphilin 3A-like (without C2 domains) [EAW90671], RPH3AL (AIC55601) and RABPHILIN-3A [Rattus norvegicus] (1ZBD_B) CDS. The QMEAN Z-score of the EAW90671 is -2.57,i.e., the score of the structure is clearly within the expected quality range as it deviates less than 1 standard deviation from the mean score in similar sized high-quality proteins from the reference dataset. The structure of the EAW90671, AIC55601, and the 1ZBD_B has a QMEAN score deviating by more than 3 standard deviations indicating that there is clearly something wrong with this structure. Both the composite QMEAN score, as well as all individual terms deviate strongly from expected values. Indeed, these structures, have been identified as fabricated and have been retracted. Higher QMEAN Z-scores in a pairwise comparison with their homologous, underlining the significance of the QMEAN Z-score as an estimate of protein stability [28].

Table 2: Z-score analysis of the EAW90671, AIC55601, and the 1ZBD_B

PDB	QMEAN	C-β	All-atom	Solvation	Torsion
EAW90671	-2.57	-0.31	-1.82	-1.80	-1.75
AIC55601	-1.43	-0.15	-0.37	-1.57	-1.17
1ZBD_B	-0.07	-0.19	-0.67	-1.36	-0.60

The QMEAN Z-scores as well as the Z-scores of individual statistical potential terms are reported. The structure has been retracted from the PDB. The QMEAN Z-score of -2.57 for EAW90671, -1.43for AIC55601 and -0.07 for 1ZBD_B in isolation is unfavourable, especially the solvation and the C-β interaction terms exhibit large differences between the Z-score of the isolates (Table 3) [28].

Higher QMEAN Z-scores in a pairwise comparison with their homologous, underlining the significance of the QMEAN Z-score as an estimate of protein stability [28].

Figure 8: QMEAN scores (-2.57) for biological unit reference set of Rabphilin 3A-like (without C2 domains) [EAW90671]. Plot showing Z-score.

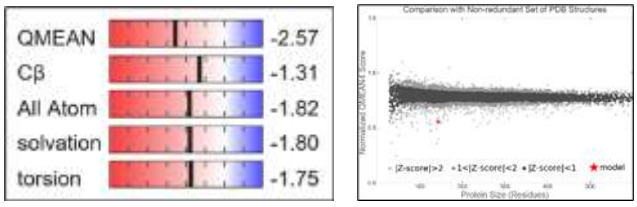

Volume 9, Issue 2; March-April 2026; Page No 419-427

Figure 9: QMEAN scores (-1.43) for biological unit reference set of RPH3AL (AIC55601) . Plot showing Z-score.

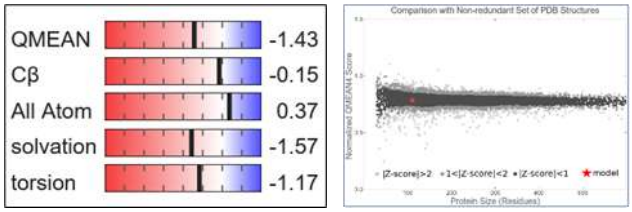

Figure 10: QMEAN scores -0.07) for biological unit reference set of 1ZBD_B. Plot showing Z-score.

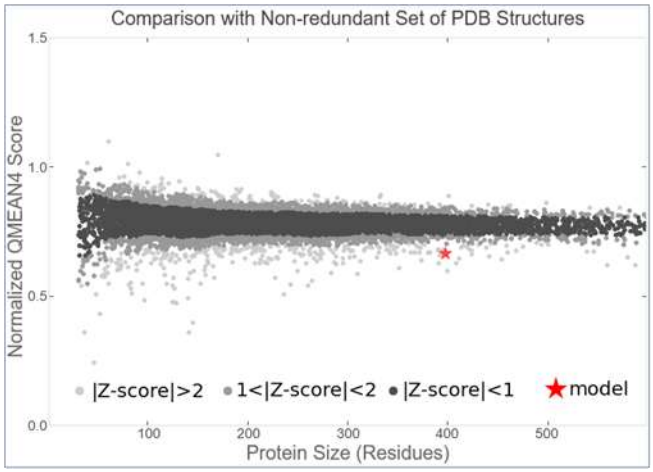

The QMEAN value comparison with the non-redundant protein collection revealed different set of Z-values for different parameters. The diversion of total energy of protein was measured by using Z-score [29, 30].

Alzheimer's disease (AD) and Huntington's disease (HD) are progressive neurodegenerative disorders that share several pathological features, particularly synaptic dysfunction and impaired neurotransmission. In both diseases, disruption of synaptic vesicle trafficking and exocytosis can lead to early neuronal communication defects before significant neuronal loss occurs. Proteins such as Rabphilin-3A-like (RPH3AL), which regulate membrane trafficking and synaptic vesicle release, may contribute to these shared mechanisms. However, the diseases differ in their causes and clinical manifestations. Alzheimer's disease primarily causes memory loss and cognitive decline, whereas Huntington's disease is a genetic disorder characterized by motor dysfunction, psychiatric symptoms, and degeneration of basal ganglia neurons.

Conclusion

In the present study, the structural characteristics of Rabphilin-3A-like isoform CRA_b (EAW90671) and RPH3AL (AIC55601), encoded by the Rabphilin-3A-like (RF3 or RPH3A) gene, were successfully predicted using an *in silico* homology modelling approach. The generated three-dimensional models exhibited strong stereochemical integrity and structural reliability, as demonstrated by favourable φ-ψ plot distributions, acceptable ProSA Z-scores, and QMEAN quality assessments.

Comparative structural analysis revealed substantial similarity between the predicted human RPH3AL models and the experimentally resolved Rabphilin-3A structure from *Rattus norvegicus*, supporting the biological relevance of the models. These findings suggest that the computationally derived structures reasonably represent the native conformations of the proteins.

Overall, this study establishes a validated structural framework for Rabphilin-3A-like proteins that can be exploited in future investigations, including inhibitory peptide design, molecular docking, and structure-based drug development. The predicted models may contribute to the identification of novel therapeutic

Volume 9, Issue 2; March-April 2026; Page No 419-427

strategies aimed at mitigating synaptic dysfunction associated with Alzheimer's disease and Huntington's disease

Financial Support

Self-finance project

Acknowledgement

The authors are grateful to Dr. P. Satyanarayana, Professor & HOD , Department of Biochemistry, Pacific Institute of Medical Sciences (PIMS), Udaipur, Rajasthan, India, for support and guidance during research work and to biochemistry and bioinformatics research group members for technical support.

Ethics Approvals

The research project was approved by the Ethics Committee (Registration no. STU/IEC/2026/005) of Pacific Institute of Medical Sciences, Sai Tirupati University, Udaipur, Rajasthan, INDIA.

References

1. Shirataki H, Kaibuchi K, Sakoda T, Kishida S, Yamaguchi T, Wada K, et al. Rabphilin-3A, a putative target protein for the Rab3A small GTP-binding protein. *Molecular and Cellular Biology*. 1993;13(4):2061-2068.
2. Geppert M, Goda Y, Stevens CF, Südhof TC. The role of Rabphilin-3A in synaptic vesicle trafficking. *Cell*. 1994;79(4):717-727.
3. Burns ME, Sasaki T, Takai Y, Augustine GJ. Rabphilin-3A: a multifunctional regulator of synaptic vesicle exocytosis. *Neuron*. 1998;20(3):523-534.
4. Südhof TC. The synaptic vesicle cycle. *Annual Review of Neuroscience*. 2004;27:509-547.
5. Selkoe DJ. Alzheimer's disease is a synaptic failure. *Science*. 2002;298(5594):789-791.
6. Li SH, Li XJ. Huntingtin-protein interactions and the pathogenesis of Huntington's disease. *Trends in Genetics*. 2004;20(3):146-154.
7. Kitchen DB, Decornez H, Furr JR, Bajorath J. Docking and scoring in virtual screening for drug discovery: methods and applications. *Nature Reviews Drug Discovery*. 2004;3(11):935-949.
8. Prajapat R, Jain S, Vaishnav MK, Sogani S. Structural Modeling and Validation of Growth/Differentiation Factor 15 [NP_004855] Associated with Pregnancy Complication-Hyperemesis Gravidarum. *JKIMSU* 2020; 9(3): 40-47.
9. Prajapat R, Marwal A, Shaikh Z, Gaur RK. Geminivirus Database (GVDB): First database of family geminiviridae and its genera Begomovirus. *Pak J Biol Sci*. 2012; 15:702-706.
10. Luthy R, Bowie JU, Eisenberg D. Assessment of protein models with three-dimensional profiles. *Nature* 1992; 356: 83-85.
11. Laskowski RA, MacArthur MW, Moss DS, Thornton JM. PROCHECK: A program to check the stereochemical quality of protein structures. *J Applied Cryst*. 1993; 26: 283-291.
12. Vriend G. WHAT IF: A molecular modeling and drug design program. *J Mol Graphics* 1990; 8: 52-56.
13. Sehgal SA, Tahir RA, Shafique S, Hassan M, Rashid S. Molecular modeling and docking analysis of CYP1A1 associated with head and neck cancer to explore its binding regions. *J Theoret Comput Sci*. 2014; 1 (3):1-6. doi: 10.4172/2376-130X.1000112
14. Agrawal P, Thakur Z, Kulharia M. Homology modeling and structural validation of tissue factor pathway inhibitor. *Bioinformation* 2013; 9: 808-812.
15. Benkert P, Tosatto SCE, Schomburg D. QMEAN: A comprehensive scoring function for model quality assessment. *Proteins: Struct Funct Bioinform*. 2008; 71: 261-277.
16. Benkert P, Kunzli M, Schwede T. QMEAN server for protein model quality estimation. *Nucleic Acids Res*. 2009; 37: W510-W514.
17. Novotny WF, Girard TJ, Miletich JP, Broze GJ. Platelets secrete a coagulation inhibitor functionally and antigenically similar to the lipoprotein associated coagulation inhibitor. *Blood* 1988; 72: 2020-2025.
18. Wiederstein M, Sippl MJ. ProSA-web: Interactive web service for the recognition of errors in three-dimensional structures of proteins. *Nucleic Acids Res*. 2007; 35: W407-W410.

Volume 9, Issue 2; March-April 2026; Page No 419-427

19. Jaiswal G, Kumar V. *In-silico* design of a potential inhibitor of SARS-CoV-2 S protein. *PLoS ONE* 2020; 15(10): e0240004.

20. Bowie JU, Luthy R, Eisenberg D. A method to identify protein sequences that fold into a known three-dimensional structure. *Science* 1991; 253: 164-170.

21. Mustufa MMA, Chandra S, Wajid S. Homology modeling and molecular docking analysis of human RAC-alpha serine/threonine protein kinase. *Int J Pharma Bio Sci*. 2014; 5: 1033-1042.

22. Rekik I, Chaabene Z, Grubb CD, Drira N, Cheour F, Elleuch A. *In silico* characterization and molecular modeling of double-strand break repair protein MRE11 from Phoenix dactylifera v deglet nour. Theor. *Biol Med Model* 2015; 12:23. doi: 10.1186/s12976-015-0013-2.

23. Berman HM, et al. The Protein Data Bank, *Nucleic Acids Res*. 2000; 28: 235-242.

24. Benkert P, Biasini M, Schwede T. Toward the estimation of the absolute quality of individual protein structure models. *Bioinformatics* 2011; 27(3): 343–350.

25. Studer G, Rempfer C, Waterhouse AM, Gumienny G, Haas J, Schwede T. QMEANDisCo - distance constraints applied on model quality estimation. *Bioinformatics* 2020; 36: 1765-1771.

26. Aires-de-Sousa M. Hemmer JG. Prediction of ^{1}H NMR Chemical Shifts Using Neural Networks. *Analytical Chemistry* 2002; 74(1): 80-90.

27. Wiederstein M, Sippl MJ. Protein sequence randomization: Efficient estimation of protein stability using knowledge-based potentials. *J Mol Biol*. 2005; 345: 1199-1212.

28. Gao J, Lu G, Qi J, Li Y, Wu Y, Deng Y, Geng H, Li H, Wang Q, Xiao H, Tan W, Yan J, Gao GF. Structure of the fusion core and inhibition of fusion by a heptad repeat peptide derived from the S protein of Middle East respiratory syndrome coronavirus. *J Virol* 2013; 87(24):13134-40. doi: 10.1128/JVI.02433-13.

29. National Center for Biotechnology Information (2022). PubChem Compound Summary for CID24139.https://pubchem.ncbi.nlm.nih.gov/compound/2-acetamido-2-deoxy-beta-D-glucopyranose.

30. Lokhande KB, Doiphode S, Vyas R, Swamy KV. Molecular docking and simulation studies on SARS-CoV-2 Mpro reveals Mitoxantrone, Leucovorin, Birinapant, and Dynasore as potent drugs against COVID-19. *J Biomol Struct Dyn*. 2020; 1-12. doi:10.1080/07391102.2020.1805019.

Volume 9, Issue 2; March-April 2026; Page No 419-427